Temperature dependence of the emission cross section of Nd:YVO4 around 1064 nm and consequences on laser operation

Xavier Délen, François Balembois, Patrick Georges

Temperature dependence of the emission cross section of Nd:YVO$_4$ around 1064 nm and consequences on laser operation

Xavier Délen,* François Balembois, and Patrick Georges

Laboratoire Charles Fabry de l'Institut d'Optique, CNRS, Université Paris-Sud,
Campus Polytechnique, RD 128, 91127 Palaiseau Cedex, France
*Corresponding author: xavier.delen@institutoptique.fr

We propose an accurate measurement of the evolution of the emission cross section of Nd:YVO$_4$ versus temperature around 1064 nm. This was done by using two complementary methods involving spectrum acquisition and laser oscillator small signal gain measurement. We observed a 44% decrease of the peak emission cross section for a 64 °C temperature increase but also a shift of the peak emission cross section wavelength at a rate of 3 pm/°C. The influence of the crystal temperature on the performance of a laser oscillator in continuous wave was also investigated.   © 2011 Optical Society of America

OCIS codes: 140.3530, 140.3580.

1. INTRODUCTION

Over the past decades, Nd^{3+} doped crystals have been widely used in diode-pumped solid-state laser setups [1,2]. Among this family of laser materials, Nd:YVO$_4$ is especially appreciated for its high emission cross section and high absorption cross section. Many high-power laser systems using Nd:YVO$_4$ under pump power above 50 W have been demonstrated [3–7]. Even if the thermal load can be reduced by using 880 or 888 nm pumping instead of the most common 808 nm pumping, the relatively high quantum defect of at least 17% (for a laser operation at 1064 nm when pumped at 888 nm) and moderate thermal conductivity result in high temperature increases under high pumping power. Although the effects of the pump-induced temperature gradients and the resulting thermal lensing have been intensively studied, only few data are available on the effect of the absolute temperature increase of the laser medium. Previous studies have shown that maximal temperatures reached in Nd:YVO$_4$ crystals under diode pumping can easily be above 100 °C [8,9]. Other papers have mentioned a significant impact of temperature on Nd:YVO$_4$ spectroscopic properties and on laser performance. A laser wavelength shift and an output power decrease have been observed by Mingxin *et al.* while tuning the temperature of a microchip laser between 0 °C and 100 °C [10]. The emission line broadening with temperature and its shift toward a higher wavelength has been measured for temperatures ranging from −263 °C to 27 °C and explained by phonon theory by Sardar and Yow [11]. More recently, the emission cross section and the central wavelength versus temperature have been studied from the spectroscopic point of view over a wide range of temperatures between −263 °C and 77 °C by Turri *et al.* [12]. However, there are only a few points of interest over the usual laser operation temperature range. Moreover, data concerning the wavelength shift are very different from one paper to the other, varying from 2 pm/°C [12] to 4.7 pm/°C [10]. It is worth noting that these papers are either

about only spectroscopy or about only lasers, but none of them link the two.

In this paper, we propose an accurate measurement of the emission cross section using two complementary methods involving spectrum acquisition but also laser parameter investigation. The effects of the temperature increase of Nd:YVO$_4$ on its spectroscopic properties and its consequences on laser operation around 1064 nm were investigated in detail. First, the evolution of the stimulated emission cross section with temperature was obtained using the Fuchtbauer–Ladenburg technique in order to acquire detailed data over the usual laser operation temperature range. Using the same setup, the small signal gain, the continuous wave (CW) output power, and the laser spectrum have been measured as a function of temperature. Then, these results are compared with the emission cross section evolution measurements and are used to check the validity of our measurement method. In the conclusion, we discuss the impact of the evolution of the spectroscopic properties with temperature on a high-power laser based on Nd:YVO$_4$ crystals.

2. INFLUENCE OF TEMPERATURE ON THE EMISSION CROSS SECTION AROUND 1064 NM

The evolution of the emission cross section spectrum versus temperature can be measured indirectly by using fluorescence spectrum, optical index, radiative lifetime evolution, and the Fuchtbauer–Ladenburg equation [Eq. (1)] [13]. Using the linear fit given by Turri *et al.* [12] for the evolution (between −73 °C and 77 °C) of the emission cross section at 1064 nm for π polarization generally used for laser action, we can anticipate a decrease of the order of 25% of the emission cross section over the temperature range in consideration, which is between 16 °C and 80 °C, corresponding to the range of our analysis. The optical index variation over 64 °C being much smaller than 0.1%, it can be considered as constant for the

emission cross section calculation. In order to limit the thermal load and to avoid nonradiative processes, we chose a low doping concentration of 0.1%. Using a Ti:sapphire pulsed excitation laser emitting around 808 nm, an interferential filter at 1064 nm, and a photodiode, we measured the evolution of the fluorescence lifetime with the crystal temperature. Between 16 °C and 80 °C, we found the fluorescence lifetime to be constant within our $\pm 1\%$ uncertainty range and equal to 98 μs. Owing the low doping concentration of our sample (0.1%), the difference between fluorescence lifetime and radiative lifetime can be neglected. Therefore, we can consider that the radiative lifetime τ_{rad} stays constant over the range of temperature aimed at in this work. As shown by Eq. (1), the variation of the cross section with temperature is, thus, only induced by the evolution of the fluorescence spectrum $I(\lambda)$:

$$\sigma_{EM}(\lambda) = \frac{(\bar{\lambda})^4}{8 \cdot \pi \cdot c \cdot n^2 \cdot \tau_{rad}} \frac{I(\lambda)}{\int I(\lambda) \mathrm{d}\lambda}. \quad (1)$$

The optical index is denoted n, c is the speed of light in vacuum, and $\bar{\lambda}$ is the average emission wavelength.

The experimental setup used in order to measure the fluorescence spectrum is described in Fig. 1. A laser diode emitting around 808 nm and coupled to a 100 μm core diameter fiber has been used as a pump source. Using a single doublet, the 5 W pump beam was focused over a 500 μm diameter spot. The laser crystal used for our experiments was an a-cut, 0.1% doped, $3\,\mathrm{mm} \times 3\mathrm{mm} \times 5\,\mathrm{mm}$ Nd^{3+} doped YVO$_4$ crystal. It was placed between two copper blocks, through which temperature-regulated water was circulating. A water boiler allowed us to set the crystal mount temperature between 16 °C and 80 °C. The use of a low pump power and a low doping concentration guaranteed a minimal pump-induced temperature increase. A thermal infrared camera and a ZnSe beam splitter were used to check this assumption. The experimental setup was similar to the one used by Didierjean *et al.* [9]. A maximal pump-induced temperature increase of 4 °C was found for 5 W pump power. This temperature rise has been neglected later on and the crystal temperature was considered to be equal to the mount temperature. Two simple lenses with a focal length of 70 mm and a polarizer beam splitter were used to collect the π-polarized fluorescence. The spectrum was only monitored for this polarization because it corresponds to the polarization
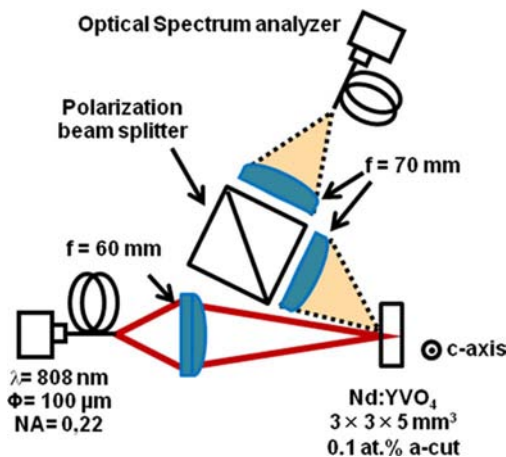

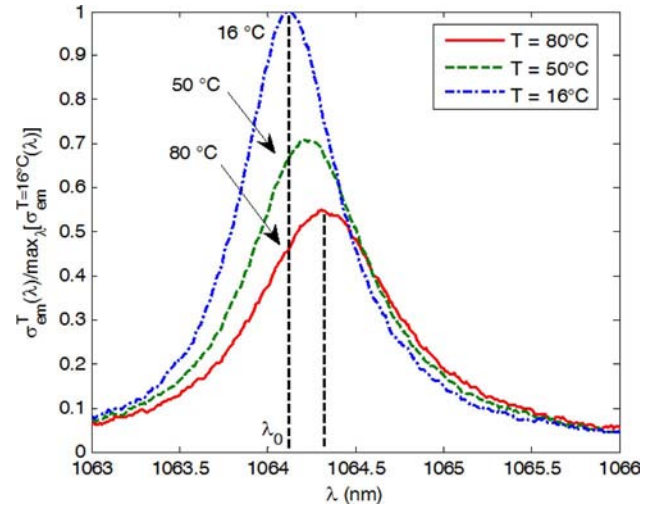Fig. 1. (Color online) Experimental setup used for fluorescence spectra acquisition.

Fig. 2. (Color online) Relative emission-cross section spectrum around 1064 nm versus temperature.

of most common Nd:YVO$_4$ lasers. A 0.07 nm resolution bandwidth optical spectrum analyzer gave the fluorescence spectrum around 1064 nm. The evolution of the spectrally integrated fluorescence intensity was measured using a photodiode placed instead of the optical spectrum analyzer.

A total of 14 different spectra have been acquired for temperatures ranging from 16 °C to 80 °C. The integrated fluorescence intensity over the whole spectrum was found to decrease by less than 2% over our range of temperature. Figure 2 shows the normalized emission cross section spectrum σ_{em} for mount temperatures T of 16 °C, 50 °C, and 80 °C. It was normalized by the maximum of σ_{em} at 16 °C. It clearly shows the decrease of the peak emission cross section, the line broadening, and the line shift toward higher wavelengths for increasing temperatures. The normalized values of maximal emission cross sections as a function of temperature $\max[\sigma_{em}(T)]/\max[\sigma_{em}(16\,°C)]$ are given in Fig. 3. The overall 64 °C temperature increase results in a 44% peak emission cross section decrease. Over the studied range of temperatures, the average decrease rate of the peak emission

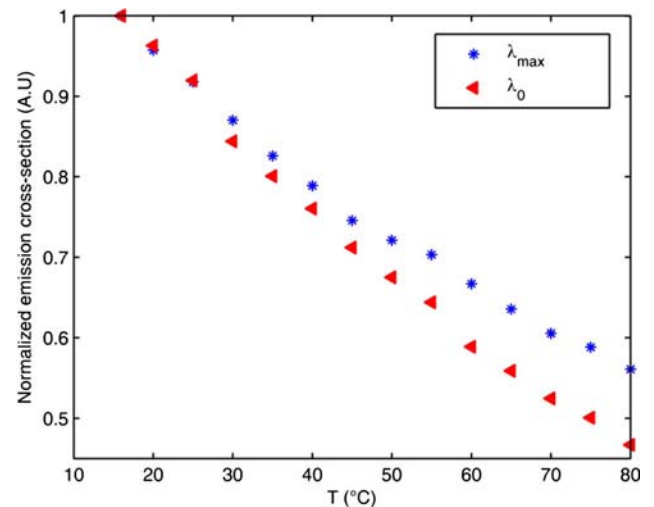Fig. 3. (Color online) Relative value of the emission cross section versus temperature. Maximal value $\max[\sigma_{em}(T)]/\max[\sigma_{em}(16\,°C)]$ and value for a fixed wavelength λ_0 corresponding to the peak emission cross section at 16 °C $\sigma_{em}(\lambda_0, T)/\max[\sigma_{em}(16\,°C)]$.
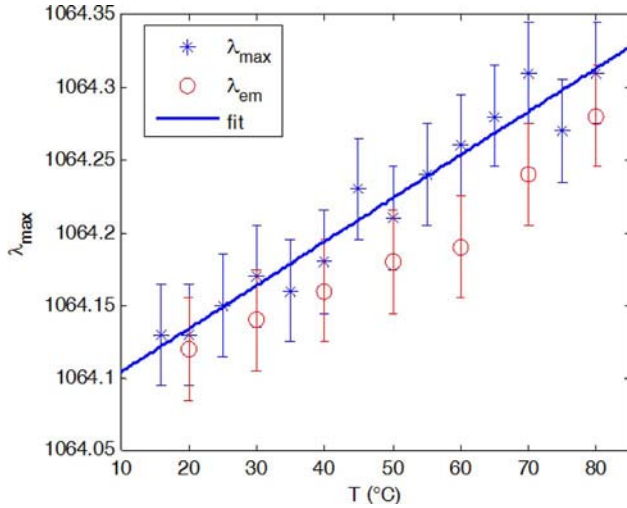
Fig. 4. (Color online) Maximal emission-cross section wavelength (blue) and laser emission wavelength (red) versus temperature (see Section 3).

cross section is about 7% per 10 °C. The evolution of the emission cross section at a fixed wavelength λ_0 is also shown in Fig. 3. λ_0 corresponds to the peak emission cross section wavelength at 16 °C. Over the whole temperature range, a 55% decrease is observed. This higher decrease is due to the combination of both the wavelength shift of the peak cross section and its decrease with temperature.

The peak emission cross section decrease that has been measured in this work is significantly higher than the 25% decrease that can be deduced from the equation given by Turri *et al.* This could be explained by the wide range of temperature for which the linear fit equation is given in their work.

As shown in Fig. 4, the wavelength of the maximal emission cross section evolves quasi-linearly between 16 °C and 80 °C. The wavelength increase rate is about 3 pm/°C, which is lower than the value found by Mingxin *et al.* [10] of 4.7 pm/°C between 0 °C and 100 °C with a microchip laser, but is higher than the average 2 pm/°C found by Turri *et al.* between −73 °C and 77 °C [12]. However, our result is very close to 2.8 pm/°C, which can be calculated from Sardar and Yow's data for Nd:YVO$_4$ between −73 °C and 27 °C [11].

As there is a discrepancy between our results and the results already published, we decided to complete this spectroscopic study with an investigation of the laser parameters versus temperature.

3. SMALL SIGNAL GAIN AND CW REGIME

We designed an experimental setup in order to investigate both the influence of the crystal temperature on small signal gain and on the output power in the CW regime. This allows an accurate comparison between the results for the two regimes. Figure 5 shows the laser cavity used for this purpose. The laser crystal and the crystal mount were kept the same as for the spectroscopic measurement. The pump beam was focused over a 250 μm diameter spot in the middle of the crystal using two doublets. The laser cavity consisted of three mirrors M$_1$, M$_2$, and M$_3$. M$_1$ was a plane dichroïc mirror with high reflectivity around 1064 nm and high transmission around 808 nm. M$_2$ was a +300 mm concave mirror highly reflective around 1064 nm and M$_3$ was a 25% transmission plane output coupler. In order to obtain a laser beam size matching the pump beam
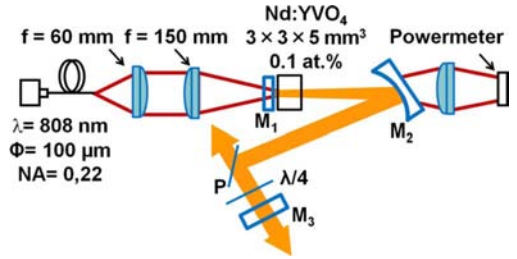

Fig. 5. (Color online) Experimental setup used for small signal gain and CW measurements. P stands for polarizer and $\lambda/4$ for quarter-wave plate.

size, we chose the following distances between the mirrors: M$_1$–M$_2$ = 210 mm and M$_2$–M$_3$ = 400 mm. The use of a linear polarizer and a quarter-wave plate in the cavity allowed a simple adjustment of the overall cavity losses by rotating the quarter-wave plate. In other words, the linear polarizer with the quarter-wave plate and the output coupler can be seen as a virtual output coupler for which the transmission T_{eq} can be chosen between 25% and 100% by rotation of the quarter-wave plate. Therefore, the output coupling value of our cavity could easily be changed without realignment. This setup reduces the sources of uncertainty for the measurement of oscillation threshold and output power versus the output coupling in comparison with a setup for which the output mirror needs to be changed and realigned carefully. Finding the coupling value T_{eq} corresponding to the threshold gives a value of the double-pass small signal gain G_0^2 using Eq. (2). δ are the passive losses of the cavity, evaluated at around 1% in our case. Our setup allowed us to record the small signal gain versus the absorbed pump power:

$$G_0^2(1 - T_{eq})(1 - \delta) = 1. \tag{2}$$

By using a lens to collect part of the residual pump power behind mirror M$_2$, the absorbed pump power was measured for each experimental condition. This measurement is necessary in order to obtain accurate data because the absorption cross section in the crystal depends on temperature but also on the pump power density (saturation of absorption) and on the laser intensity. Figure 6 shows the double-pass small signal gain measured as a function of the absorbed pump power P_{abs} for three different crystal temperatures T. In our configuration, a 60 °C temperature increase results in a dramatic reduction of the double-pass small signal gain from 12 to 4.5 for about 1.75 W of absorbed pump power.

This result can be compared with the spectroscopic measurements obtained in Section 2. Following gain calculation for longitudinal pumping with a cylindrical symmetry [14], it can be shown that the double-pass small signal gain G_0 is

$$G_0^2(P_{abs}, T) = \exp\{K \max[\sigma_{em}(T)]P_{abs}\}, \tag{3}$$

where K is a quantity that is independent of the temperature but function of the overlap between pump and signal beams. P_{abs} is the total absorbed pump power, $\max[\sigma_{em}(T)]$ is the peak emission cross section versus wavelength assuming that the small signal gain is always measured at the wavelength corresponding to the maximum. The product $K \max[\sigma_{em}(16\,°C)]$ is adjusted by fitting the gain curve at 16 °C. The solid line gain curves at $T = 45\,°C$ and $T = 80\,°C$
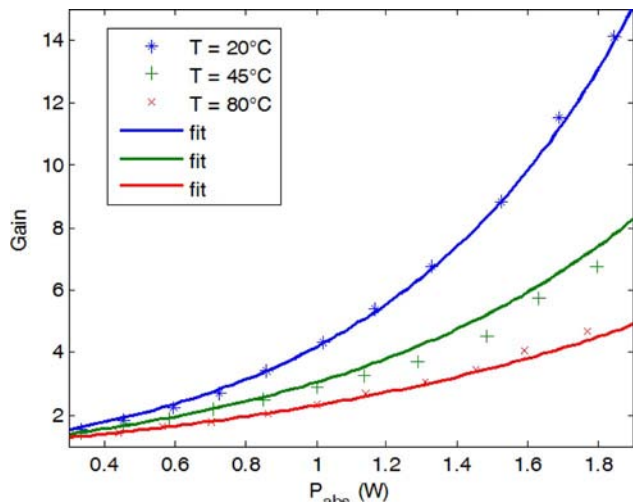
Fig. 6.   (Color online) Double-pass small signal gain as a function of the absorbed pump power for three different crystal temperatures. Solid curves, exponential fit for 20 °C, modeling for 45 °C and 80 °C.

were calculated using the data of the peak emission cross section versus temperature (from Fig. 2) and the fitting parameter for 16 °C. It shows a good agreement between measured gain values and calculated values. This clearly indicates that the gain decrease observed can be attributed to the decrease of the peak emission cross section with temperature. In fact, our double-pass small signal gain measurement could also be a method for measuring the relative evolution of the peak emission cross section with the temperature of the crystal.

For an output coupler of 25% transmission, the emission wavelength as a function of temperature has been acquired in CW using the same optical spectrum analyzer as for the fluorescence spectrum acquisition. The results are shown in Fig. 4, together with the wavelength corresponding to the peak emission cross section. It appears clearly that, according to the theory, the emission wavelength follows the peak emission cross section wavelength. The shifting rate is identical and equal to 3 pm/°C. We are working with a long cavity that has a free spectral range very small compared to the emission line width. This is not the case for the very short cavities involved when a microchip laser is used. It probably explains why the microchip laser emission wavelength shift of
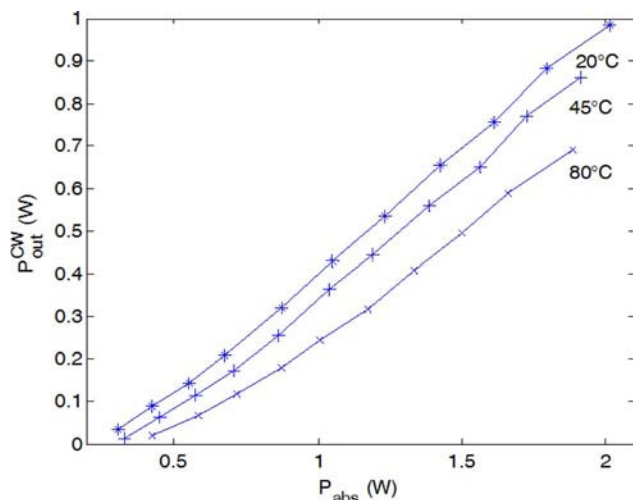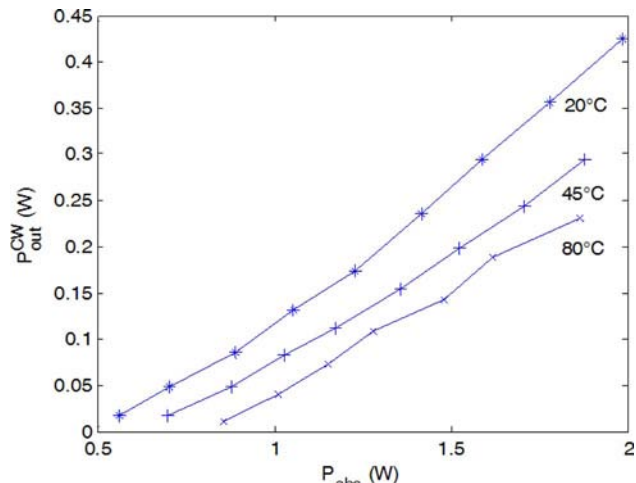

Fig. 8.   (Color online) Efficiency curves for 50% coupling and crystal temperatures of 20 °C, 45 °C, and 80 °C.

4.7 pm/°C observed by Mingxin *et al.* is large compared to our value.

Using the setup used for small signal gain measurement and taking into account the total output power coming from the polarizer and M_3, we measured the efficiency curves for different coupling values and crystal temperatures in CW regime. Figures 7–9 show the set of data obtained for transmissions of 25%, 50%, and 75% for temperatures of 16 °C, 45 °C, and 80 °C. The absorbed pump power threshold shift with temperature is larger for high coupling values. For example, with a coupling value of 25%, the threshold increases by less than 200 mW, whereas for a 75% coupling value, it increases by over 650 mW. As expected, the emission cross section decrease with temperature leads to a threshold increase. Note that the small signal gain curves give threshold values matching the values observed experimentally. The temperature impact on the output power is also clearly visible. Whereas, for low coupling values, the impact of the temperature increase stays modest, it has a dramatic impact on the output power for high coupling values. For example, the decreases in output power are, respectively, about −25%, −40%, and over −70% for coupling values of 25%, 50%, and 75%. The emission cross section decrease is not the only explanation for the lower output

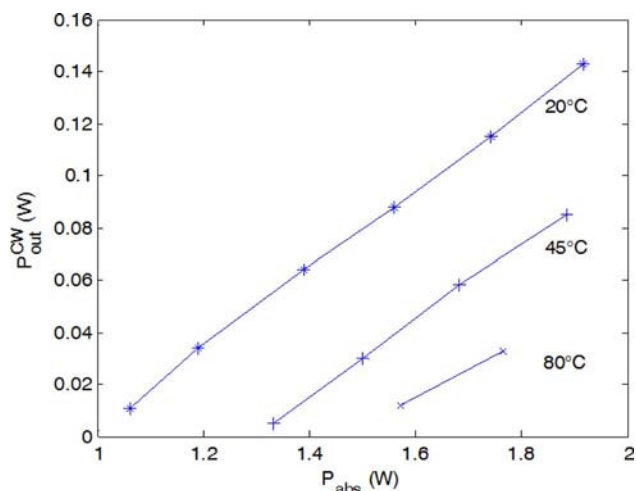

Fig. 7.   (Color online) Efficiency curves in the CW regime for 25% coupling and crystal temperatures of 20 °C, 45 °C, and 80 °C.

Fig. 9.   (Color online) Efficiency curves for 75% coupling and crystal temperatures of 20 °C, 45 °C, and 80 °C.

power obtained at higher temperatures: as we are working with a linear cavity with a gain medium at one end, we suspect spatial hole burning to be responsible for gain inhomogeneities resulting in the slope efficiency decrease. In any case, a reduction of the temperature results in improved performance in the CW regime, especially for high output coupling values.

4. DISCUSSION AND CONCLUSION

We present here a set of accurate measurements of spectroscopic and laser parameters for Nd:YVO$_4$ for a temperature range corresponding to the classical crystal temperatures under laser operation. The measurement of the emission cross section decrease of 44% between 16 °C and 80 °C is confirmed by small signal gain measurements. The wavelength shift of 3 pm/°C is also confirmed by the wavelength shift in CW laser operation.

According to previous studies on other Nd-doped crystals, the peak emission cross section decrease over our range of temperature is between 10% and 12% for Nd:YAG [15,16], which is over 3 times less than the values we obtained for Nd:YVO$_4$. A 13% decrease between 16 °C and 80 °C and a 2.6% decrease, respectively, can be calculated from literature data for Nd:GSGG and Nd^{3+} doped phosphate glass [16,17]. In conclusion, it seems that the decrease rate of the emission cross section is particularly high for Nd:YVO$_4$ when compared to other Nd^{3+} doped crystals.

Concerning the wavelength shift, the literature reports a wavelength shift of 4.5 pm/°C for temperatures ranging from 50 °C to 275 °C for Nd:YAG [18]. A similar value of 4 pm/°C has been found for Nd/Cr:YAG by Saiki *et al.* between 50 °C and 200 °C [19]. In conclusion, the value found experimentally shows a shifting rate about 25% lower for Nd:YVO$_4$ than for Nd:YAG.

As shown in previous studies, the crystal temperature can strongly influence laser performance [18,20]. The emission cross section decrease with temperature can not only affect the output power in the CW regime, but can also influence key parameters, such as pulse duration in a Q-switched regime. This effect seems to be particularly important for Nd:YVO$_4$ when compared to other Nd^{3+} doped crystals. Hence, designing a Nd:YVO$_4$ high-power laser system does not only involve managing thermal lensing and crystal cooling, but also involves working with laser crystals having lower performance due to the absolute temperature increase. In the case of a longitudinal temperature gradient, the peak emission cross section spectral shift might result in an inhomogeneous gain broadening and also result in an overall gain reduction. Furthermore, Nd:YVO$_4$ based MOPA system performance can also be strongly reduced by a temperature difference between the oscillator and the amplifier because of the emission line shift.

REFERENCES

1. G. Huber, C. Krankel, and K. Petermann, "Solid-state lasers: status and future," J. Opt. Soc. Am. B **27**, B93–B105 (2010).

2. J. Hecht, "Short history of laser development," Appl. Opt. **49**, F99–F122 (2010).

3. L. McDonagh, R. Wallenstein, and A. Nebel, "111 W, 110 MHz repetition-rate, passively mode-locked TEM00 Nd:YVO$_4$ master oscillator power amplifier pumped at 888 nm," Opt. Lett. **32**, 1259–1261 (2007).

4. M. Luhrmann, C. Theobald, R. Wallenstein, and J. A. L'Huillier, "High energy cw-diode pumped Nd:YVO$_4$ regenerative amplifier with efficient second harmonic generation," Opt. Express **17**, 22761–22766 (2009).

5. Q. Liu, X. P. Yan, X. Fu, M. L. Gong, and D. S. Wang, "183 W TEM00 mode acoustic-optic Q-switched MOPA laser at 850 kHz," Opt. Express **17**, 5636–5644 (2009).

6. X. P. Yan, Q. Liu, X. Fu, H. L. Chen, M. L. Gong, and D. S. Wang, "High repetition rate dual-rod acousto-optics Q-switched composite Nd:YVO$_4$ laser," Opt. Express **17**, 21956–21968 (2009).

7. P. Zhu, D. J. Li, P. X. Hu, A. Schell, P. Shi, C. R. Haas, N. A. L. Wu, and K. M. Du, "High efficiency 165 W near-diffraction-limited Nd:YVO$_4$ slab oscillator pumped at 880 nm," Opt. Lett. **33**, 1930–1932 (2008).

8. J. Didierjean, S. Forget, S. Chenais, F. Druon, F. Balembois, P. Georges, K. Altmann, and C. Pflaum, "High resolution absolute temperature mapping of laser crystals in diode-end-pumped configuration," Proc. SPIE **5707**, 370–379 (2005).

9. J. Didierjean, E. Herault, F. Balembois, and P. Georges, "Thermal conductivity measurements of laser crystals by infrared thermography. Application to Nd: doped crystals," Opt. Express **16**, 8995–9010 (2008).

10. Q. Mingxin, D. J. Booth, G. W. Baxter, and G. C. Bowkett, "Performance of a Nd:YVO$_4$ microchip laser with continuous-wave pumping at wavelengths between 741 and 825 nm," Appl. Opt. **32**, 2085–2086 (1993).

11. D. K. Sardar, and R. M. Yow, "Stark components of F-4(3/2), I-4(9/2) and I-4(11/2) manifold energy levels and effects of temperature on the laser transition of Nd^{3+} in YVO$_4$," Opt. Mater. **14**, 5–11 (2000).

12. G. Turri, H. P. Jenssen, F. Cornacchia, M. Tonelli, and M. Bassi, "Temperature-dependent stimulated emission cross section in Nd^{3+}:YVO$_4$ crystals," J. Opt. Soc. Am. B **26**, 2084–2088 (2009).

13. B. Aull and H. Jenssen, "Vibronic interactions in Nd:YAG resulting in nonreciprocity of absorption and stimulated emission cross sections," IEEE J. Quantum Electron. **18**, 925–930 (1982).

14. F. Balembois, F. Falcoz, F. Kerboull, F. Druon, P. Georges, and A. Brun, "Theoretical and experimental investigations of small-signal gain for a diode-pumped Q-Switched Cr:LiSAF laser," IEEE J. Quantum Electron. **33**, 269–278 (1997).

15. J. Dong, A. Rapaport, M. Bass, F. Szipocs, and K. Ueda, "Temperature-dependent stimulated emission cross section and concentration quenching in highly doped Nd^{3+}:YAG crystals," Phys. Status Solidi A **202**, 2565–2573 (2005).

16. A. Rapaport, S. Z. Zhao, G. H. Xiao, A. Howard, and M. Bass, "Temperature dependence of the 1.06 μm stimulated emission cross section of neodymium in YAG and in GSGG," Appl. Opt. **41**, 7052–7057 (2002).

17. J. Dong, M. Bass, and C. Walters, "Temperature-dependent stimulated-emission cross section and concentration quenching in Nd^{3+}-doped phosphate glasses," J. Opt. Soc. Am. B **21**, 454–457 (2004).

18. O. Kimmelma, I. Tittonen, and S. C. Buchter, "Thermal tuning of laser pulse parameters in passively Q-switched Nd:YAG lasers," Appl. Opt. **47**, 4262–4266 (2008).

19. T. Saiki, K. Funahashi, S. Motokoshi, K. Imasaki, K. Fujioka, H. Fujita, M. Nakatsuka, and C. Yamanaka, "Temperature characteristics of small signal gain for Nd/Cr:YAG ceramic lasers," Opt. Commun. **282**, 614–616 (2009).

20. M. Bass, L. S. Weichman, S. Vigil, and B. K. Brickeen, "The temperature dependence of Nd^{3+} doped solid-state lasers," IEEE J. Quantum Electron. **39**, 741–748 (2003).